On the Effects of Wet Underwater Welding on the Fracture Behaviour of Welds

Lutz Lindhorst, TÜV Süddeutschland Bau und Betrieb GmbH, Munich, Germany

ABSTRACT

The influence of the water contact during wet underwater welding on the crack tip opening displacement (CTOD) is investigated in this paper. The welding process is numerically simulated. An example of a welded rectangular plate is presented. The power density distribution of the welding process is determined and the instationary temperature field during welding and cooling is calculated. The microstructural changes are considered as well as the welding residual stress distribution which remains in the structure after the cooling process is finished. The welding residual stresses are applied on a fracture specimen. The mechanical material properties of the heat affected zone of the weld due to microstructural changes during welding and cooling are implemented in the fracture model. The CTOD is determined in an elastic-plastic fracture mechanics analysis for a sharp, stationary crack on the surface of a bead on plate weld under bending. The calculations are carried out using the finite-element-method (FEM). The results of a wet underwater welding process are compared to those of a dry welding process.

INTRODUCTION

Wet underwater welding is established as an important technology for building and maintaining ships and off-shore equipment. But there are further areas where underwater welding can be used. The nuclear power industry has been identified as one of these areas. Underwater welding offers advantages for the repair and decommissioning of components or equipment which must be kept under water due to reasons of radiation or contamination. But until now, the application of wet underwater welding on load carrying components is restricted by the weld quality, which often does not reach the quality of dry welding processes.

The quality of a weld is made up of several factors. Two such factors are the residual stresses and the microstructure. The water contact during wet underwater welding causes the material in the weld and the material surrounding the weld to cool very rapidly. This can lead to regions of high residual stresses and furthermore to unwanted changes in the microstructure. Both effects can deteriorate the mechanical properties of the weld and cracks can occur. As a result, the fracture mechanics of underwater welds are an area of concern. Though there are many data on fracture parameters of cracks under various loading conditions, only few deal with cracks under residual stresses or material inhomogeneity caused by underwater welding.

WELDING PROCESS

The Plasma-MIG welding technique (1) is investigated in this paper. A schematic of the process is shown in Fig. 1.

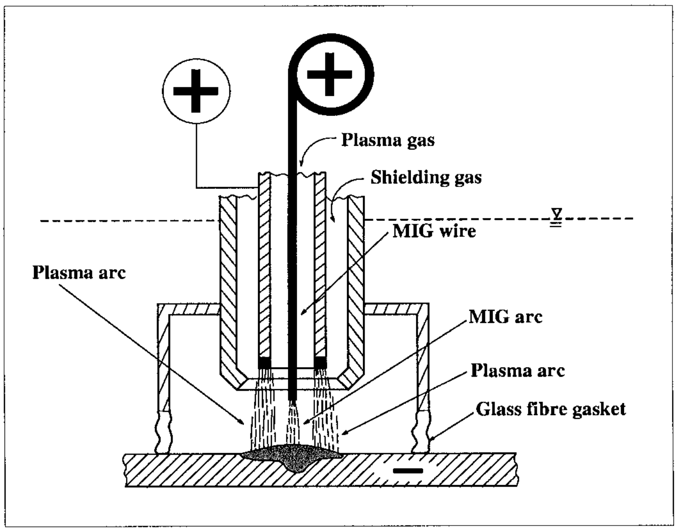

Figure 1: Plasma-MIG Welding Technique

This technique is a combination of Plasma and MIG welding. Both belong to the "Direct Light" processes. The Plasma-MIG technique uses a mechanically fed fusible metal electrode. It is suitable for welding in air atmosphere and under water. In case of underwater welding, it works as a dry spot underwater welding method with a local stabilized gas volume around the weld zone. The heat is created by the discharge of electrical energy when the positive and the negative electrode come in contact with each other. The positive electrode is the weld wire, which is fed at constant velocity to the welding head as the weld progresses. The ground, or negative electrode, is the weld specimen. The heat released from both the Plasma arc and the MIG arc melt the wire as well as the base metal.

The MIG arc is surrounded by a region of hot inert gases. These gases protect the weld from the environment, in water and in the air. The heat transfer from the arcs to theses gases is heat loss. This is in the model accounted for by the efficiencies of the two arcs. The efficiency of the welder is improved by trapping inert gases between the MIG arc and the Plasma arc. The Plasma gas is ionized which improves conductivity between the two electrodes. This stabilizes the Plasma arc, which in turn creates a weld that transfers material to the weld specimen without splattering.

An example of Plasma-MIG welding of a bead on plate weld is presented in this paper. The dimension of the weld specimen is shown in Fig. 2.

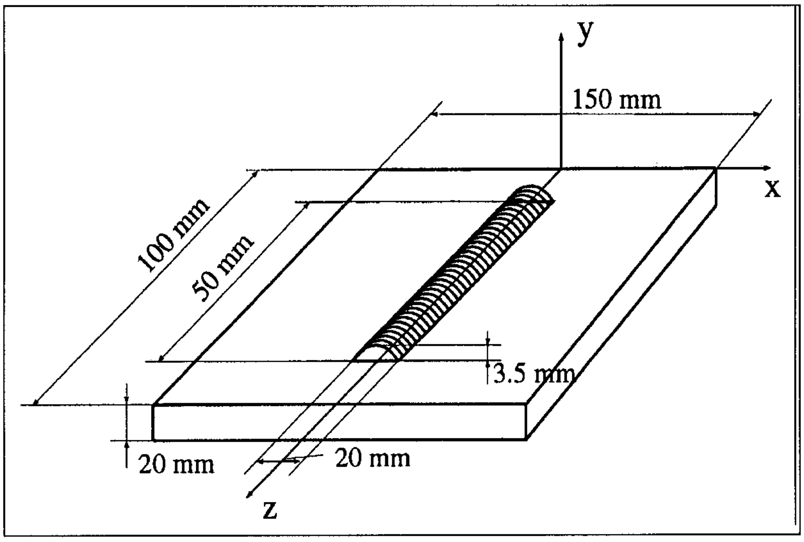

Figure 2: Dimension of the Welded Plate

NUMERICAL SIMULATION OF WELDING

A numerical model presented by Hamann & Mahrenholtz (2; 3) is used to determine the heat flux input by the two arcs. The heat flux of the arcs is approximated by a hemispherical (MIG arc) and a two dimensional (Plasma arc) power distribution. The welding parameters of the process are listed in table 1.

Table 1: Welding Parameters of Plasma and MIG Arc for the Bead on Plate Weld

	MIG	Plasma
current	250 A	200 A
voltage	28 V	35 V
efficiency	0.60	0.65
diameter water free zone	90 mm	
velocity	3.42 mm/s	

The material transfer of the MIG arc is considered in the FE model of the plate (Fig. 3). The corresponding FE elements are fused at the start of the welding process. They are activated during simulation according to the local positions of the arcs.

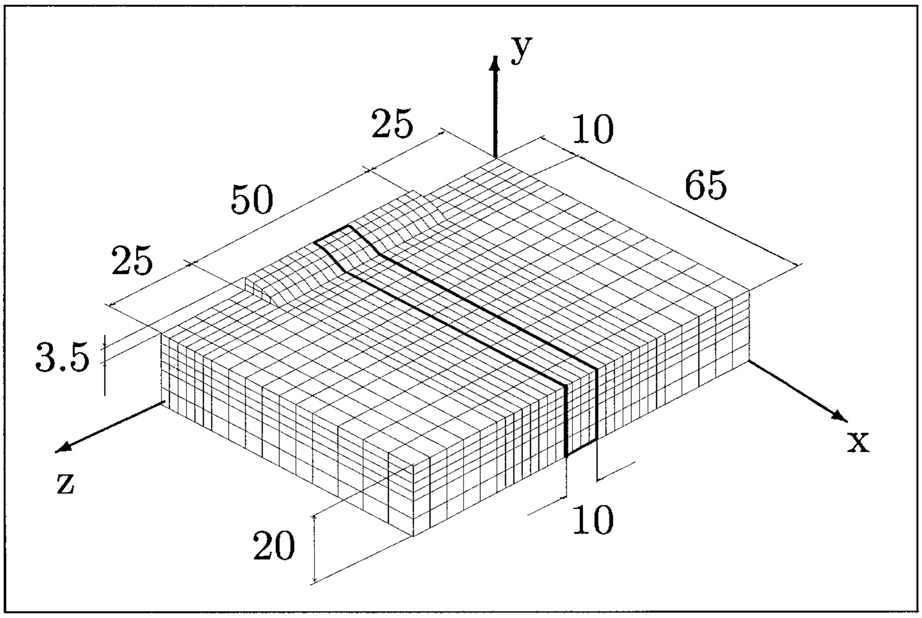

Figure 3: FE-Half-Model of the Welded Plate

Different analysis are performed in order to show the influence of the water contact on fracture parameters of wet welds. A wet underwater welding process and a dry welding process (air atmosphere) using the Plasma-MIG welding technique are investigated. The results of the wet welding process are compared to those of the dry welding process. The instationary temperature field during welding is calculated and used to determine the welding residual stress distribution that remains after cooling is finished.

The weld specimen is a rectangular plate with a dimension of 100 mm x 150 mm x 20 mm (Fig. 2). A bead on plate weld of 50 mm length and 20 mm width is welded on the surface of the rectangular plate. The symmetry of the structure is taken into account and a three dimensional FE half model is used. The model consists of 3020 eight-noded isoparametric brick elements with 3836 nodes. The instationary temperature field during welding and the residual stress distribution after cooling are calculated with this model (Fig. 3).

The fracture analysis is performed for a three point bend specimen extracted from the welded plate. The geometry of the fracture specimen and the crack geometry are presented in Fig. 4. The fracture specimen is cut out of the center of the initial plate shown in Fig. 2. The material in this simulation is the StE 355.

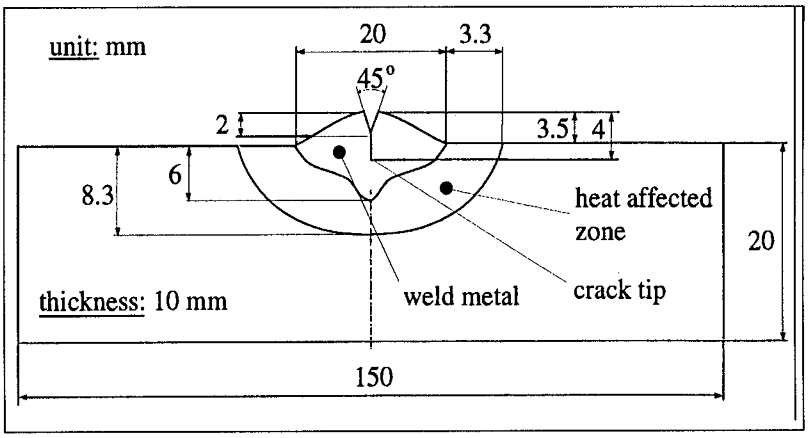

Figure 4: Geometry of the Fracture Specimen

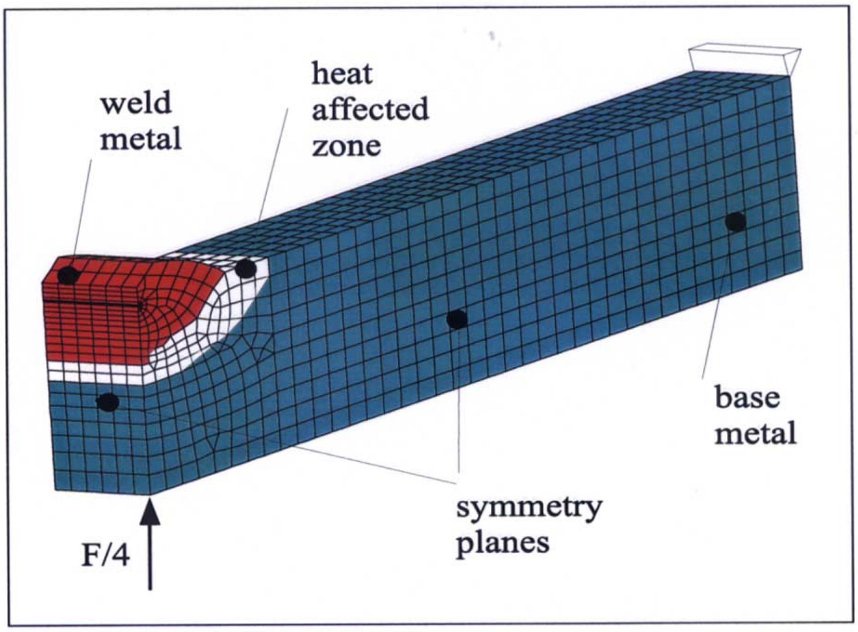

Figure 5: FE Discretization (Quarter Model) of the Fracture Specimen

TEMPERATURE FIELD

Whether the environmental conditions have an important influence on the temperature distribution or not depends on the surrounding fluid. The water contact during wet underwater welding influences mainly the temperature distribution in the welded body. Hamann et al. (3) have investigated the influence of the water contact on the temperature field. They have developed a model to determine the surface heat transfer coefficient. This model takes into account material effects, orientation of the surface and the influence of undercooled boiling. This model is used to calculate the surface heat transfer to water for the wet underwater welding process.

The calculation of the instationary temperature field is separated into the problems of heat conduction, heat transfer to environment and simulation of welding process. The heat conduction problem is solved numerically due to the nonlinear, temperature dependent material properties. The internal energy accumulated by the deformation of the body is negligibly small for the heat conduction problem of a conventional arc welding process (4). The balance of the internal energy for such a process is described by the Fourier heat conduction equation. The time integration is performed by using the unconditionally stable Dupont II scheme (5).

WELDING RESIDUAL STRESSES

There are two physical mechanisms causing residual stresses during welding. The first of them is the inhomogeneous volume change due to local heating and cooling. It leads to elastic stresses and to plastic deformation. Stresses set up after the temperature field is balanced are referred to as thermal residual stresses. The second mechanism is phase transformation leading to local volume changes and transformation stresses. These two types of stresses are equal from the mechanical point of view (6).

The thermal loads due to heat input by the two moving arcs are gradually applied on the specimen in the FE analysis in order to determine the elastic and plastic strains. The total strain increment is given by the sum of the elastic, the plastic, the creep, the thermal and the strain increment due to phase transformation.

The creep strain increment is not determined but neglected because of the high cooling rate during wet underwater welding. The calculation of the strain increment due to phase transformation requires a coupled thermo-mechanical-metallurgical model and the temperature dependent material properties have to be considered. The welding residual stresses are calculated using an elastic plastic material law with multilinear isotropic hardening rule.

PHASE TRANSFORMATIONS

The model used in this investigation is based on a method presented by Leblond et al. (7; 8). With this model, the phase distribution that occurs in the weld after cooling is finished is determined considering the austenite, ferrite, perlite, bainite and martensite phases. The mechanical material properties of the heat affected zone are calculated according to the distribution of the different phases in the weld and transferred into the model of the fracture specimen (9). A comparison between different methodologies for calculation of phase transformations in welding processes is given in (10).

FRACTURE ANALYSIS

The fracture analysis is performed with the specimen shown in Fig. 4. The crack is located in the center of the weld parallel to the welding direction with 4 mm crack length. Fig. 5 shows the FE discretization of the fracture specimen. The fracture analysis is complicated for the steep stress gradient that occurs in the vicinity of the crack tip. The crack tip stress singularity dictates the use of a fine FE mesh in this region (11). Therefore a three-dimensional FE mesh is set up consisting of twenty-noded isoparametric elements (Fig. 5). The symmetry of the structure is taken into account and a quarter model is used. Prismatic elements are defined at the crack tip with one element for every 30^o in the circumferential direction. The singularity at the crack tip is modelled using twenty-noded Quarter-Point elements. One line of each element at the crack tip is collapsed. The collapsed lines are coupled at the crack tip node. The transition of the mesh from very small elements (about 5% of the crack length) at the crack tip to larger elements in areas away from the crack is achieved by dividing the regions with prismatic elements.

The welding residual stresses calculated for the plate shown in Fig. 2 and 3 are applied on the fracture specimen using nodal forces. Three different material zones are considered (Fig. 5), the weld metal, the heat affected zone and and the base metal. The values of the mechanical material parameters of the weld metal and the heat affected zone are determined in the calculation of the phase transformations. The dimensions of the volumes of the weld metal and the heat affected zone are taken from the temperature field calculation. Thereby, a fracture model is build up, which considers residual stresses as well as material heterogeneity.

The crack tip opening displacement CTOD-δ_5 (12) is calculated with this model under static loading. An elastic plastic material behaviour with multilinear isotropic hardening is assumed in the fracture analysis.

RESULTS

The results of the welding simulation and the fracture analysis are shown with examples in Fig. 6 and 7. Fig. 6 presents the temperature distribution in the dry weld and the wet weld at simulation time t=16.25 s. Fig. 7 shows a comparison between CTOD-F-curves of the fracture specimens extracted from the wet and the dry welded plate.

Differences in the size of the molten pool occur between the wet and the dry weld (Fig. 6) due to the different environmental conditions of the two welding processes. The molten pool of the dry weld is about 15 mm longer (in welding direction) as that of the wet weld. There are only slight differences in the depth and width of the molten pool (perpendicular to welding direction). The water contact contact during wet underwater welding leads to a high cooling rate compared to that of dry welding in air atmosphere. The temperature gradient in the vicinity of the weld seam is approximately 140 $^oC/mm$ (dry weld) and about 170 $^oC/mm$ (wet weld). These differences in the temperature gradient and cooling velocity of the two plates lead to different welding residual stress distributions and material properties as well.

As a result, the CTOD-F-curve presented in Fig. 7 shows the effect of the different boundary conditions (cooling in air atmosphere and under water) on the crack tip opening displacement. The gradient of the wet weld curve is higher than that of the dry weld curve between CTOD=0 mm and CTOD=0.09 mm. This is due to the different mechanical properties in the weld metal and heat affected zone of the wet and dry welded specimen. It leads to lower CTOD values of the wet weld than those of the dry weld in the first part of the CTOD-F-curve, if the CTOD values for both boundary conditions are regarded at the same external load F. For CTOD values larger than 0.09 mm, the gradient of the wet weld curve is smaller than that of the dry weld curve. The fracture of the wet weld will occur at smaller external load and at smaller CTOD than those of the dry weld, which is caused by the deteriorated mechanical properties of the wet weld compared to that of the dry weld and by the interaction of external load and residual stresses.

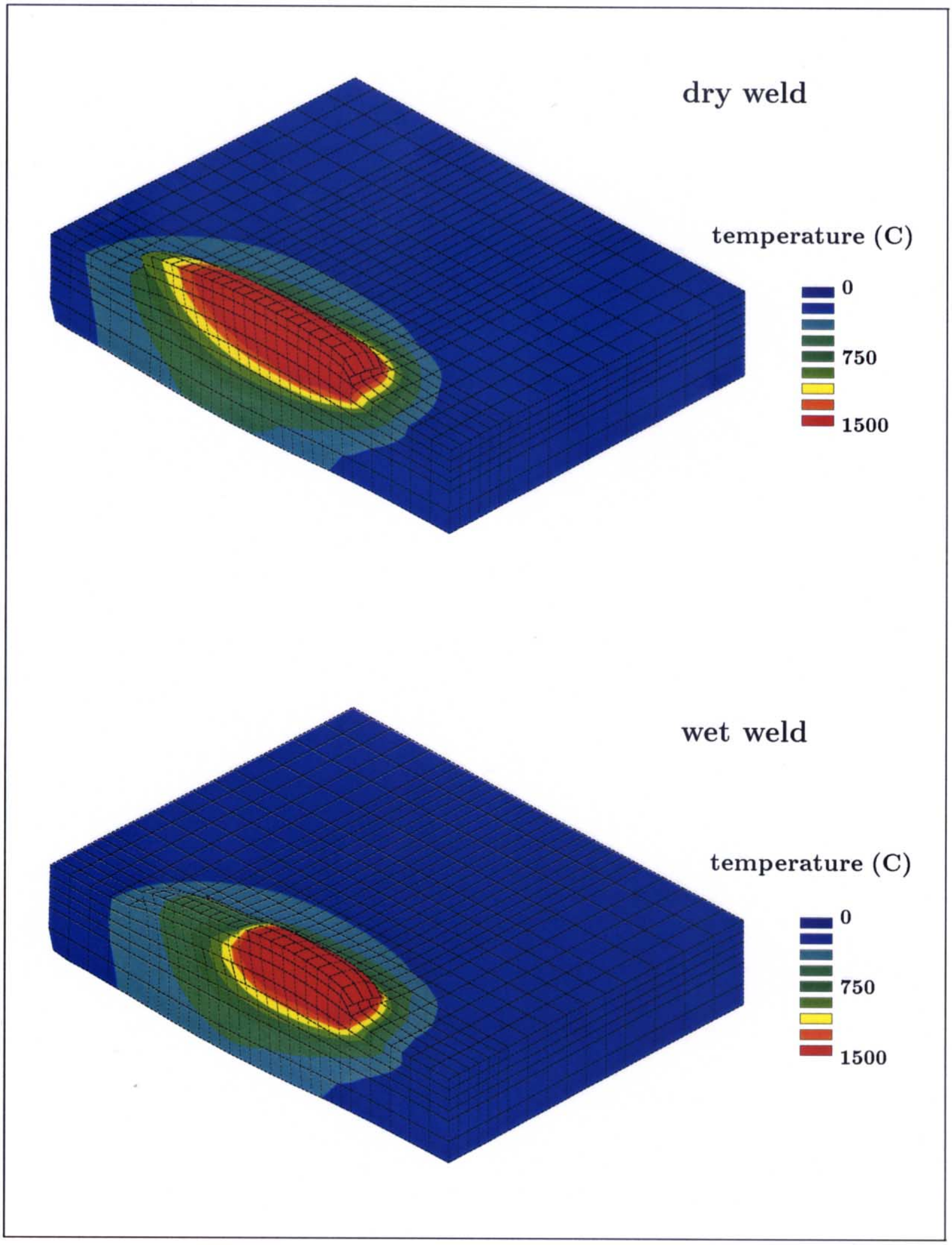

Figure 6: Temperature Field of Wet Weld and Dry Weld (time=16.25 s)

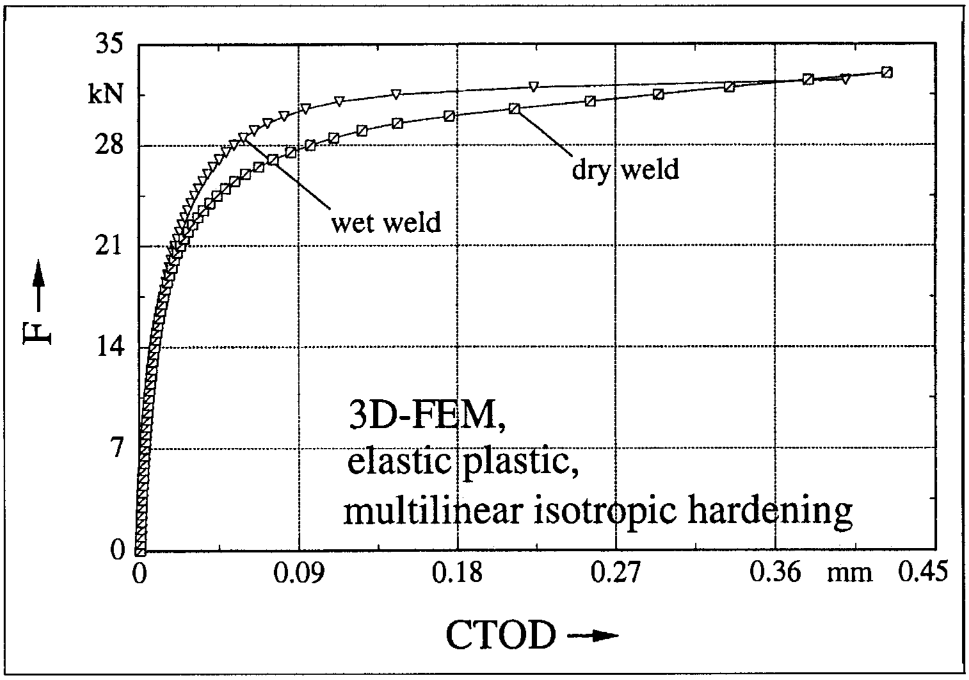

Figure 7: CTOD-F-Curve, Comparison between Wet Weld and Dry Weld

CONCLUSIONS

The influence of the water contact on CTOD is investigated in this paper regarding the Plasma-MIG underwater welding process. The welding process is numerically simulated and an example of a dry and wet welded bead on plate weld is presented. The power density distribution of the welding process and the instationary temperature field during welding and cooling are calculated. The microstructural changes and the welding residual stresses resulting from the instationary temperature field are considered in the fracture model. The CTOD is determined in an elastic-plastic fracture mechanics analysis for a sharp, stationary crack on the surface of a bead on plate weld under bending. The calculations are carried out using the FEM.

The results presented show that the instationary temperature field is mainly influenced by the water contact in case of wet underwater welding. The water contact leads to a high cooling velocity and to a high temperature gradient in the vicinity of the weld seam compared to dry welding in air atmosphere. The differences in the temperature field of the two processes influence the residual stresses and material heterogeneity in the welded plates. The results of the fracture analysis obtained with three-point-bend specimens extracted from the welded plates show, that the CTOD is influenced by the water contact in case of wet underwater welding. The different residual stresses and material heterogeneity contribute to the deteriorated CTOD-curve of the wet weld compared to that of the dry weld.

In this example, the quality of the wet weld does not reach the quality of the dry weld. Therefore, further investigations on the influence of the water contact in Plasma-MIG underwater welding are necessary in order to improve its applicability on load carrying components.

REFERENCES

1. Draugelates, U. ; Bouaifi, B. ; Bartzsch, J. 1993: Underwater welding using Plasma MIG method. Int. Conf. on Offshore Mechanics And Arctic Engineering (OMAE), vol. 4. IIIA.

2. Hamann, R. ; Mahrenholtz, O. 1994: On the influence of the surface heat transfer coefficient on wet underwater welds. Int. Offshore and Polar Engineering Conf. (ISOPE), vol. 4.

3. Hamann, R. ; Mahrenholtz, O. ; Bartzsch, J. 1992: Temperature Distribution of Wet Underwater Welding. Int. Offshore and Polar Engineering Conf. (ISOPE), vol. 4.

4. Banas, A. ; Hsu, T.R. ; Sun, N.S. 1987: Coupled thermoelastic-plastic stress analysis of solids by finite element method. Journal of Thermal Stresses, 10 (4), 319–345.

5. Hogge, M. 1981: Numerical Methods in Heat Transfer. J. Wiley & Sons. Chap. 4, 75 – 90.

6. Wu, Chuan Song. 1992: Computer simulation of three-dimensional convection in travelling MIG weld pools. Engineering Computations (Swansea, Wales), 9 (5), 529–537.

7. Leblond, J.B. ; Deveaux, J. ; Deveaux, J.C. 1989a: Mathematical modelling of transformation plasticity in steels I: Case of ideal–plastic phases. International Journal of Plasticity, 5, S.551–572.

8. Leblond, J.B. ; Deveaux, J. ; Deveaux, J.C. 1989b: Mathematical modelling of transformation plasticity in steels II: Coupling with strain hardening Phenomena. International Journal of Plasticity, 5, S.573–591.

9. Lindhorst, L. 1999: Numerische Simulation des Plasma-MIG-Unterwasserschweissens - Eigenspannungen, Gefuege und Bruchmechanik. VDI Fortschrittberichte, Reihe 2, Nr. 499.

10. Mahrenholtz, O. ; Lindhorst, L. ; Ronda, J. ; Oliver, G.J. 1997: Comparison of welding residual stresses in a dry and a wet underwater Plasma-MIG weld. International Conference on Residual Stresses, Linkoeping, Sweden.

11. Kuo, A.-Y. ; Tang, S.S. ; Yu, T.P. 1993: Thermally induced stress intensity factor of a semi-circular surface crack in a half-space. International Journal of Fracture, 62, 219–232.

12. Schwalbe, K.-H. 1980: Bruchmechanik metallischer Werkstoffe. Carl Hanser Verlag, München.